Liquid Film Dynamic on the Spray Impingement Modelling

C. Rodrigues, J. Barata and A. Silva*
Dept. of Aerospace Science, University of Beira Interior, Covilhã, Portugal
christian23_rodrigues@hotmail.com, jbarata@ubi.pt, andre@ubi.pt

Abstract

The present paper addresses a liquid film sub-model included into a computational model that aims at reproducing the spray impingement phenomena. This numerical extension incorporates the spread of the liquid film over the neighbouring nodes due to the dynamic motion induced by the film inertia but also the exchange of mass between the liquid layer and the incident and splashing particles. Moreover, the dimensionless film thickness parameter is introduced into the sub-model by mean of an experimentally-deduced correlation that can be fitted and updated to specified conditions. In order to realize how the model behaves with different influencing parameters, a thorough investigation is performed: the results that are obtained with and without the liquid film sub-model are compared against the experimental data for two crossflow rates. The integration of the computational extension with the spread/splash transition criterion is also evaluated by considering two types of transition criteria: one that takes into account the effect of the film thickness and one that does not. The results show that the latter option in combination with the sub-model do not distinctly enhance the simulation results, contrary to what happens using the transition criterion that considers the film thickness as an influencing parameter. In this case, the model with the computational extension reveals better prediction results than the one without it, which indicates the necessity of considering the liquid film formation for spray impingement simulations but also a splash threshold that takes into account the influence of the film thickness.

Introduction

The dynamic of droplets impacting onto a dry or wet solid surface plays an important role in a wide variety of fields, such as in ink-jet printing technologies, spray painting and coating, raindrops impacting on the ground and in liquid-fuelled combustors. However, it has only been in the near decade that a major scientific effort has been pursued in order to acquire a detailed and comprehensive knowledge about the mechanisms underlying the spray impingement process. Yet, this complete physical understanding is still lacking due to the host of parameters that influence the outcome. One of those parameters, which, curiously, is often neglected in spray impingement models, is the liquid film accumulated on the wall due to the deposition of the incident drops.

The correct understanding of the film dynamic is of utmost importance for the accurate modelling of the spray impingement phenomenon. In fact, it is a key influencing parameter in several specific applications: if, on the one hand it is important to avoid as far as possible the liquid layer over the surface in situation of diesel engines cold-starting, on the other hand the presence of this liquid film is desired in cooling systems applications. In a general way, the formation of a liquid film and its interaction with the incident spray strongly affects the mixing process by taking effect on such properties as the splashing threshold and the secondary droplets characteristics.

Despite the new boundary conditions promoted by the liquid/liquid interaction, the surface characteristics may still have significant influence on the outcome depending on the thickness of the film [1]. In fact, given the depth of the liquid over the solid surface, Tropea and Marengo [2] considered four categories (very thin film, thin film, thick film and deep pool) in which they defined a dependence between the influence of the surface topography and the dimensionless film thickness (ratio of the film liquid thickness to the incident drop diameter). The authors found that only in the case of a deep pool, which is not the condition reported in this study, the impact depend neither on the surface roughness nor on the film thickness.

The present work aims at developing and integrating a liquid film extension in a multiphase computational model. This paper follows on from a set of previous studies [3–5] that seek to refine a flexible dispersion model in some aspects that would allow converging towards the best computational solution with minimum time constraints through the use of adapted and more suitable empirical correlation that fit specific configurations. Therefore, the liquid film formation sub-model is proposed by considering some basic principles (conservation of mass and volume between impinging and adhered parcels) but also an empirical correlation deduced from experimental data [6] for the average film thickness which allows a connection to the phenomenological experience that can easily be fitted and updated to specific settings. This model is incorporated into the code originally proposed by Bai et al. [7],

*Corresponding author: andre@ubi.pt

which has meanwhile been modified and improved (see Ref. [5]), and the performance is recognized through the comparison between the numerical results - with and without the liquid layer - and the measurements for two crossflow rates. In addition, two transition criteria between the deposition and splash regimes are considered: the first one concerns the expression proposed by Bai et al. [7], whereas the second has been chosen from a previous study in which it was found that the transition criterion suggested by Cossali et al. [8] presented better results for the size distributions of the upward moving droplet when integrated into this numerical simulation. It is also worth mentioning that only the latter boundary threshold takes into account directly the influence of the liquid film in the correlation embedded into the dispersion model. This situation is properly reported in the following sections.

Numerical Method

Mathematical Model

The numerical predictions resulting from the computational simulation of the multiphase flow are based on an hybrid mathematical approach. The fluid phase is treated as a continuum by solving the partial differential equations in a fixed reference frame. The turbulence is modelled by mean of the well-known "k-ε" turbulence model, which was found to predict reasonably well the mean flow [9] and the QUICK scheme of Leonard [10] is used in order to evaluate the convection terms in the discretization process. The dispersed phase is treated using a Lagrangian reference frame in which the particle trajectories are obtained by solving the particle momentum equation through the Eulerian fluid velocity field.

The flow configuration is shown schematically in Fig. 1 and consists of a spray stream injected through the upper wall of a rectangular channel with an inclination of 20° (in relation to the vertical plane), in the direction of the stream flow. The cross section of the computational domain is 86 mm x 32 mm, whilst the channel length is 350 mm. The location of the injection point (Z_{in}) lies 50 mm downstream from the inlet plane (Z_{in}/H = 1.563) and on the symmetry plane. The six boundaries of the computational domain considered here are an inlet and outlet plane, a plane of symmetry and three solid walls at the top, bottom and side of the channel.

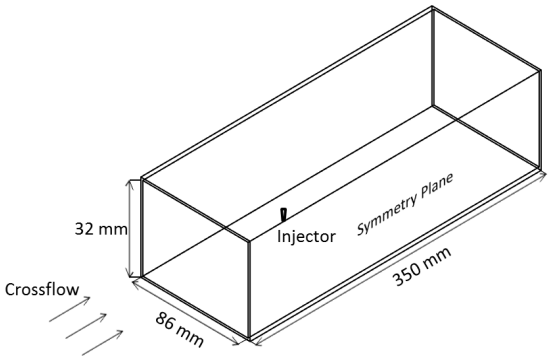

Figure 1. Schematic diagram of the flow geometry

Numerous assumptions must be made in order to allow the modelling of the droplets behaviour within an adequate time frame. In the dispersed phase, it is assumed that the particles are sufficiently dispersed so that the interaction between droplets is negligible. Considering also that the droplets are spherical and their aerodynamic breakup and evaporation can be ignored allows to establish an empirical procedure to fill a gap that prevails in the literature which is to formulate a reliable atomization model that would estimate the characteristics of the spray throughout the drops injection. Indeed, despite the fact that the measured probability density function (*pdf*) is taken in an horizontal plane located 80 mm downstream the nozzle, the three assumptions serve as a formulation basis which enables the consideration that the spray possess the same characteristics at the injector exit.

The present dispersion model, which was developed for impinging droplets onto a dry and/or wetted wall bellow the boiling temperature, is incorporated into a three-dimensional computational method based on the solution of the Reynolds-Averaged Navier-Stokes equations for the gas phase, and a SSF (stochastic separated flow) model based on eddy lifetime for the particles phase. Regarding the post-impingement characteristics resulting from secondary atomization, each impinging particle can produce up to 6 splashing parcels, each on with equal proportion of the total mass of liquid. As in Bai et al. [7] the velocity magnitudes of the secondary droplets are estimated from energy conservation while their sizes follow a Chi-squared distribution fit to experimental data and the number of droplets in each secondary parcel is determined by mass conservation.

Regimes Transition Criteria

The secondary atomization is influenced by numerous parameters that govern the droplet impingement process. Accounting for the relative importance of a set of parameters acting on the incident droplets becomes more practical if they are defined in terms of dimensionless groups. The most relevant ones, particularly for the establishment of the transition criteria defining the boundaries between different impingement regimes, are the Weber number (We = $\rho v_b^2 d_b/\sigma$), Reynolds number (Re = $\rho v_b d_b/\mu$), Ohnesorge number (Oh = $\mu/(\rho d_b \sigma)^{1/2}$) and Laplace number (La = $d_b \rho \sigma/\mu^2$), where d_b is the droplet diameter just before the impact, v_b is droplet velocity and ρ, μ, σ are the

droplet density, viscosity, and surface tension, respectively.

The model of Bai et al. [7] considers four impingement regimes: stick, rebound, spread and splash. The existence of these regimes depends on the properties of the impinging droplets and the conditions of the solid surface, including whether the latter is dry or wetted. Under any of the previous conditions, the spread-splash regime transition criteria were derived from the Stow and Hadfield data [11], giving rise to a Critical Weber number dependent on the Laplace number. The boundaries stick-rebound and rebound-spread (derived from Lee and Hanratty data [12]) for wetted walls were set with the critical Weber number of 2 and 20, respectively (see Table 1).

Table 1. Impingement regimes and corresponding transition criteria.

	Authors	**Wall Status**	**Regime Transition State**	**Critical Weber Numbers**
Original Model	Bai et al. [7]	Dry	Deposition/Splash	$We_c=2630.La^{-0.183}$
		Wetted	Stick/Rebound	$We_c=2$
			Rebound/Spread	$We_c=20$
			Spread/Splash	$We_c=1320.La^{-0.183}$
New Transition Criteria	Cossali et al. [8]	Wetted	Spread/Splash	$We_c=\frac{2100+5880\delta^{1.44}}{Oh^{-0.4}}$

A qualitative comparison of the spread/splash transition criteria for wet walls available in the literature has been performed in Ref. [3]. The experimentally-deduced correlations were inserted into a dispersion model and the results were analysed against experimental data for a specific set of boundary conditions. It was found that some transition criteria revealed an enhanced performance in some particular conditions. In fact, regarding the velocity-size correlations of the upward-moving droplets (which are mostly secondary droplets resulting from the disintegration process of the splash regime) the transition criterion of Bai et al. [7] revealed a better agreement with the measurements than the others correlations evaluated. On the other hand, in the case of the droplets size distributions of the droplet moving away from the wall, the critical threshold proposed by Cossali et al. [8] presented the best predictions. In this latter study, the authors investigated the transition between spread and splash regimes by analysing a large number of pictures of droplets impacting on an aluminium plate with a non-dimensional film thickness between 0.08 and 1.2. They found that a correlation based on the Weber and Ohnesorge numbers could fit adequately their data, as highlighted in Table 1.

Liquid Film Sub-model

A closer look at the Table 1 shows that besides the different dimensionless group used to identify the boundary between the deposition and splash regimes, which by itself corresponds to a dissimilar view of the properties affecting the disintegration process of the drops, the transition criterion proposed by Cossali et al. [8] considers the film thickness as an influencing parameter on the accurate evaluation of the critical threshold. This situation is assessed throughout this work and the results are compared against the transition criterion that does not include the effect of the film thickness (Bai et al. [7]).

The present section summarizes the main features of the liquid film formation which is presented in this work. This sub-model represents an extension to the computational model used in previous studies [3–5] to simulate the spray/wall interactions with the purpose of improving the knowledge about the spray impingement process. In fact, from that set of computational investigations, it was demonstrated that there was a clear need for a refinement of the secondary droplets treatment, particularly regarding the conditions under which the velocity profile of the parcels resulting from the splash regime were obtained. In this sense, the introduction of the liquid film upgrade gives rise to a different impingement problematic environment which alters the general outcome of the simulation.

Keeping in mind the necessity of maintain a flexible dispersion model that could be adjusted to specific boundary conditions through the use of experimental correlations that would fit those settings, the liquid film sub-model was formulated considering, besides the basic principles of volume and mass conservation, a connection to the experimental data that is given through the dimensionless film thickness. The influencing parameters of a reliable expression would relate the average film thickness to the spray characteristics and the topography of the target surface. That expression is found in Ref. [6] and is obtained from dimensional analysis. Despite the narrow and particular application range (indeed, covering - until a certain extent - the conditions of this numerical simulation) in which the expression is based on, the prediction capabilities showed good consistency with the measurements

and, thus, seemed to be a promising correlation to apply in the liquid film sub-model of the present work:

$$\bar{h} = \zeta d_{30b} Re_b^{-1/2} \left(\dot{q}/\bar{u}_b\right)^{\gamma} \tag{1}$$

where $\bar{h}$ is the deposited liquid film thickness, d_{30b} is the volumetric mean diameter of the incident particles, Re_b is the Reynold number of the incident particles, $\dot{q}$ is the flux density of the impacting spray, $\bar{u}_b$ is the averaged normal component of the impact velocity and ζ and γ are constant values that are admitted to be 4 and -0.5, respectively, as proposed originally based on the measured data.

The main features of the computational extension have to do with its capacity to deal with the interaction and the spreading of the liquid layer along and between adjacent nodes. In addition, also the splash regimes is treated carefully, whether through the consideration of the liquid/liquid interface into the impingement conditions or through the exchange of mass between the liquid film and the incident drops. On the other hand, the tangential momentum of oblique impacting drops has not been yet taken into account due to the difficulty to find a reliable expression that would accurately define the shearing forces at the interface between the liquid and the gas phases. This situation is still in progress and will certainly be subjected to further revisions in the future.

Results and Discussion

The numerical predictions presented in this section are compared and assessed with the experimental data of Arcoumanis et al. [13] (named "measurements") for two cases of crossflow velocities: 5 and 15 m/s. Two different populations of droplets are distinguished from the results presented below: one set consists of the droplets moving towards the wall while the other comprises the droplets moving in the opposite sense. In addition, two types of graphs are illustrated: the size-distributions of the droplets, which correspond to the probability density functions of the droplet size classes; and the droplet mean velocities as function of their size. Figure 2 shows the four different measurement locations where the present results are compared with the experimental data of Arcoumanis et al. [13]. The four different positions a, b, c, and d are located in the centre of the wind tunnel and lie respectively at 12, 15, 20, and 25 mm downstream of the injector and within a horizontal plane 5 mm above the impingement wall. In order to ensure brevity and conciseness of this section only the most meaningful results are revealed.

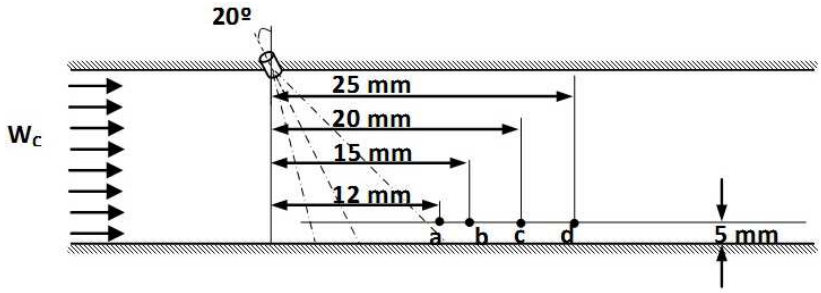

Figure 2. Illustration of the measurement locations.

Figure 3 illustrates the distribution of the relative liquid film thickness over half the impingement wall (a symmetry plane is considered at X=0) obtained with a crossflow of 15 m/s. The impact of drops with low Weber numbers lead them to coalesce and form a liquid layer on the solid surface that influences the dispersion of the droplets. The figure shows that a thin liquid film forms along the surface but has a particular incidence in the region below the nozzle, which is where the maximum thickness is found. The mixing process of the droplets is also associated with the interaction between the particles and the surrounding environment. The presence of a moving gas phase enable the appearance of a boundary layer that influences the spray/wall interactions. Due to the presence of this crossflow, the incident parcels deposit in the downstream direction, as illustrated in Fig. 3. The reduction of the air flow rate to 5 m/s leads to the thickening of the liquid film (to a maximum relative dimensionless film thickness of 0.018) and the reduction of the number of the secondary droplets resulting from the splash event. Moreover, more deposited particles are found upstream of the injector location, since the lower crossflow velocity prevents the dragging of the particles. These observations are consistent with the results reported in Ref. [14–16].

Evaluate the effective integration between the transition criterion embedded into the dispersion model, which may assume diverse types and formulations, and the computational liquid film extension that is presented in this paper becomes of utmost importance for the modelling of such flows. Therefore, the results of the simulation obtained with the splash threshold that does not include the effect of the film thickness is compared against the

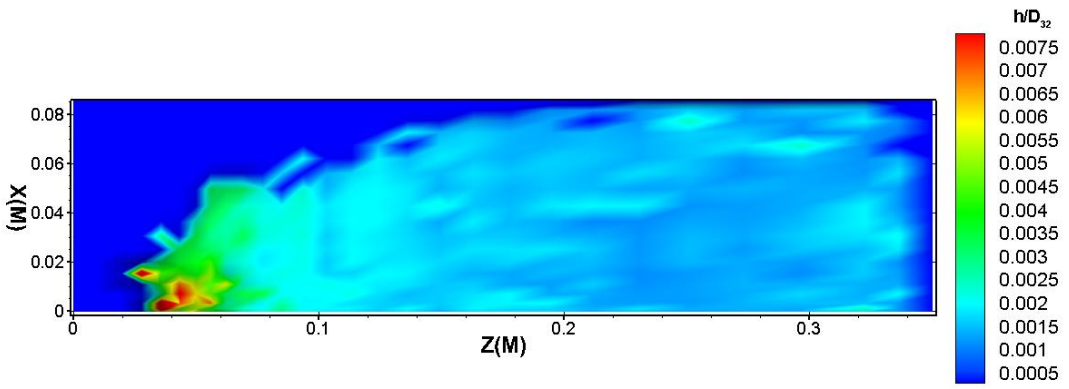

Figure 3. Distribution of the Relative Liquid Film Thickness.

one that consider it. With the former option, the results show a very similar behaviour whether considering the dispersion model without the liquid film upgrade or the one with it. Figure 4 depicts the size distributions of the upward-moving droplets with the presence of a 5 m/s crossflow where the major differences are verified between both versions. Nevertheless, a slight improvement in the new model results is noticed. In all other cases in which the transition criterion of Bai et al. [7] is employed the prediction results are even more close and thus are not presented in this paper.

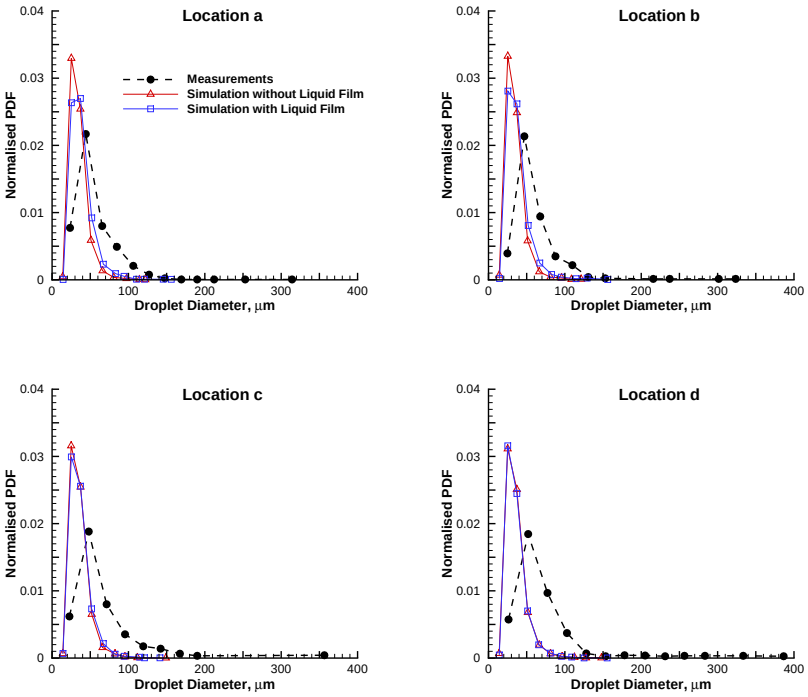

Figure 4. Size distributions of the upward-moving droplets for a crossflow velocity of 5m/s.

Regarding the results obtained with the transition criterion between the deposition and splash regimes that considers the dimensionless film thickness as an influencing parameter, the same conclusion cannot be drawn. In fact, in this group of graphs it is seen that the liquid film extension enables the achievement of prediction results that lie closer to the experimental data. The only exception is presented in Fig. 5 in which the size-distributions of the upward-moving droplet through a 5 m/s crossflow is illustrated. It can be seen that, beyond a slight leftward shift of the distribution which mean that there is a higher occurrence probability of smaller droplets moving upward, the

improved model over-estimates the mode of the droplet diameters at the four locations.

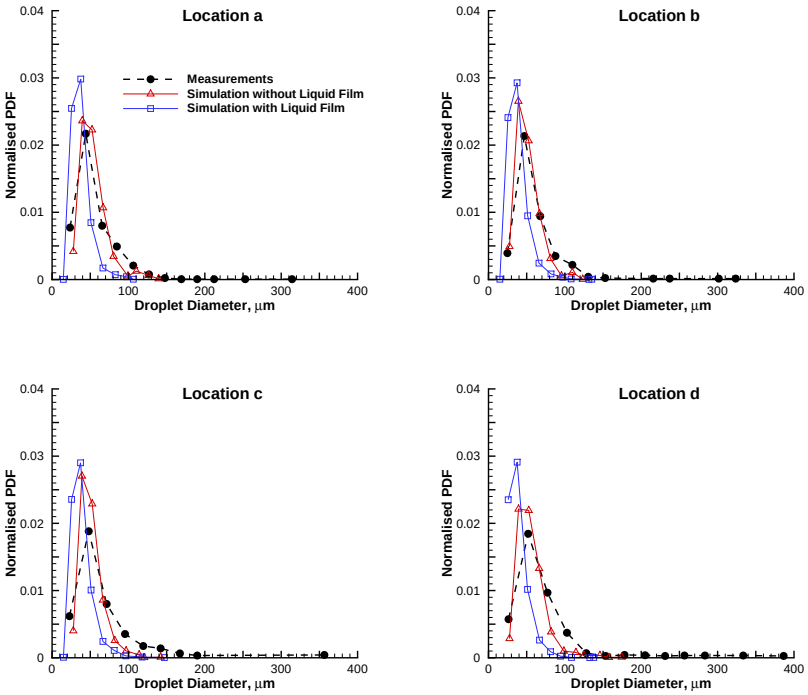

Figure 5. Size distributions of the upward-moving droplets for a crossflow velocity of 5m/s.

Besides the previous exception, the extension capabilities are quite evident in the remaining results. Figure 6 shows the size-distributions of the droplets moving towards the wall through a crossflow of 5 m/s. It is evident that the simulated results show close agreement with the measurements. This concordance is enhanced at the location further away from the injector plane for the case of the improved model: the peak value of the distribution is no longer over-estimated, as opposed to the model without the liquid film sub-model. Still, to note also that at this location there are not found any of the larger size classes which differs from measurement data. The enhancement in the numerical predictions is even more noticeable in the figures that represent the droplet mean velocities in the direction normal to the wall for the ones moving upward. In fact, as it can be seen in Figure 7 for the higher crossflow rate considered, the results of the base simulation show an over-estimation of the velocity profile at all the location (which is also increased by the use of the transition criterion of Cossali et al. [8] as referred in Ref. [3]) whereas with the model of the present work it becomes clear that the same results are improved: the predictions lie closer to the measurements.

Summary and Conclusions

The liquid film formation sub-model has been presented in this paper as an extension to the spray impingement simulation. The results are tested against experimental data and against previous numerical predictions of the same model but without the presence of the liquid film effect.

Considering the present sub-model extension, it deals with the interaction and spreading of liquid between adjacent nodes as well as the exchange of mass between the incident drops, the secondary droplets and the liquid film. In addition, in order to ensure a direct connection to experimental configurations and their corresponding data, the model allows the introduction of a correlation that relates the average film thickness accumulated on the wall to the spray characteristics and surface topography. The following conclusions can be drawn. As it would be expected, the use of a transition criterion that does not take into account the effect of the liquid layer above the impinging surface gives rise to very similar behaviours between both numerical results. In fact, in the case were the minor differences were verified revealed, nevertheless, a small improvement of the computational results obtained with liquid film extension. Integrating in the same model the effect of the presence of a liquid film with different local values of the dimensionless film thickness and a transition criterion that considers this effect on the spread/splash regime boundary allows the enhancement of the model performance. The velocity-size correlation

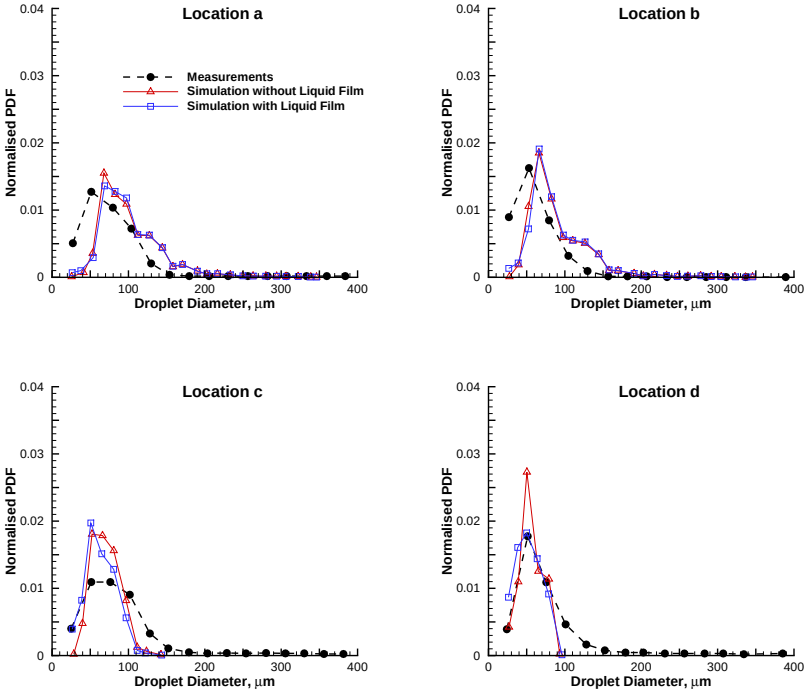

Figure 6. Size distributions of the downward-moving droplets for a crossflow velocity of 5m/s.

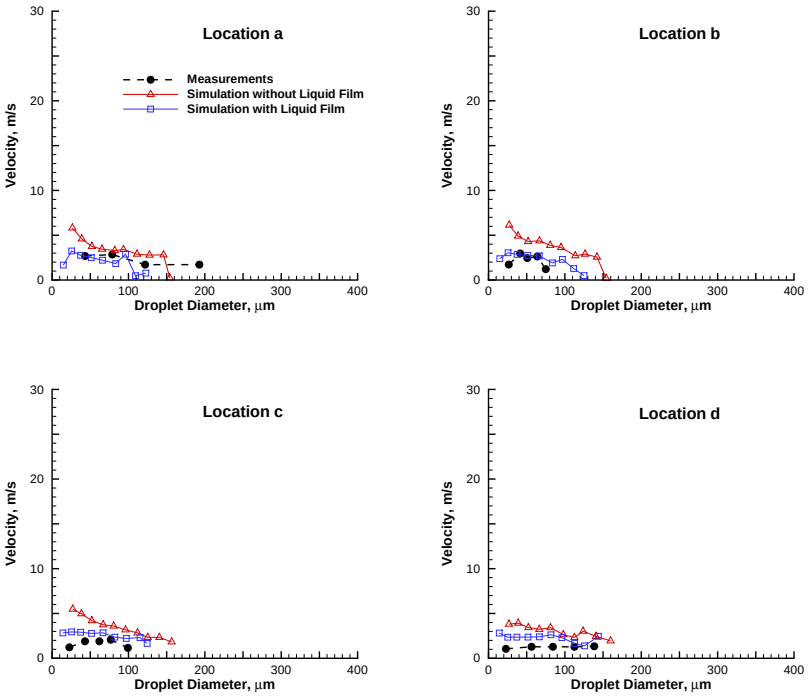

Figure 7. Velocity-size correlations of the upward-moving droplets for a crossflow velocity of 15m/s.

predictions were the results that revealed the greatest improvements, which is expectable since those graphs convey the influence of the most important parameters (from the velocity profile to the droplets size classes) and thus are more prone to be influenced by a more accurate estimation of the drops impact conditions and secondary droplets characteristics.

It is worth mentioning that the liquid film sub-model proposed in this article may still be considered as being in progress since further improvements are expected to be carried out: the principal topic that will undergo further revisions deals with the necessity of a comprehensive understanding of the liquid/gas interface, which will be of utmost importance to accurately solve the tangential momentum conservation equation.

Acknowledgements

The present work was performed under the scope of the LAETA - Laboratório Associado em Energia, Transportes e Aeronáutica - activities. C. R. thanks the Fundação para a Ciência e Tecnologia (FCT) for the financial support through the PhD Grant SFRH/BD/77651/2011.

References

[1] Randy L. Vander Wal, Gordon M. Berger, and Steven D. Mozes. The splash/non-splash boundary upon a dry surface and thin fluid film. *Experiments in Fluids*, 40(1):53–59, October 2005.

[2] C. Tropea and M. Marengo. The impact of drops on walls and films. *Multi Science Technology*, 11(1):19–36, 1999.

[3] A. Silva, J. Barata, and C. Rodrigues. Influence of Spread/splash Transition Criteria on the Spray Impingement Modelling. In *24th European Conference on Liquid Atomization and Spray Systems*, pages 1–10, 2011.

[4] C. Rodrigues, J. Barata, and A. Silva. Influence of the Energy Dissipation in the Spray Impingement Modeling. In *50th AIAA Aerospace Sciences Meeting*, pages 1–11, Nashville, Tennessee, 2012.

[5] Christian Rodrigues, Jorge Barata, and André Silva. Dissipative Energy Loss and Influence of an Enhanced Near-Wall Treatment. In *11th Int. Conference on Combustion and Energy Utilization*, pages 1–16, 2012.

[6] Davood Kalantari and Cameron Tropea. Spray impact onto flat and rigid walls: Empirical characterization and modelling. *International Journal of Multiphase Flow*, 33(5):525–544, May 2007.

[7] C. X. Bai, H. Rusche, and a. D. Gosman. Modeling of Gasoline Spray Impingement. *Atomization and Sprays*, 12(1-3):1–28, 2002.

[8] G. E. Cossali, A. Coghe, and M. Marengo. The Impact of a Single Drop on a Wetted Solid Surface. *Experiments in Fluids*, 22(6):463–472, 1997.

[9] J. Barata. Jets in Ground Effect with a Crossflow. *AIAA Journal*, 36(9):1737–1740, 1998.

[10] B. P. Leonard. A Stable and Acccurate Convective Modeling Procedure Based on Quadratic Upstream Interpolation. *Computer Methods in Applied Mechanics and Engineering*, 19(1):59–98, 1979.

[11] C. D. Stow and M. G. Hadfield. An Experimental Investigation of Fluids-Flow Resulting from the Impact of a Water Drop with an Unyielding Dry Surface. *Proc. R. Soc. Lond. A*, 373(1755):419–441, 1981.

[12] M. M. Lee and T. J. Hanratty. The Inhibition of Droplet Deposition by the Presence of a Liquid Wall Film. *International Journal of Multiphase Flow*, 14(2):129–140, 1988.

[13] C. Arcoumanis, D. S. Whitelaw, and J. H. Withelaw. Gasoline Injection Against Surface and Films. *Atomization and Sprays*, 7(4):437–456, 1997.

[14] D.F. Durão, A. L. N. Moreira, and M. R. O. Panão. The effect of a cross-flow on secondary atomization in multipoint fuel injection systems. In *13th Int Symp App Laser*, pages 1–12, Lisbon, 2006.

[15] C. Mundo, M. Sommerfield, and C. Tropea. On the Modeling of Liquid Sprays Impinging on Surfaces. *Atomization and Sprays*, 8(6):625–652, 1998.

[16] Randy L. Vander Wal, Gordon M. Berger, and Steven D. Mozes. Droplets splashing upon films of the same fluid of various depths. *Experiments in Fluids*, 40(1):33–52, October 2005.